A Real-time World-wide Ionospheric Model for Single and Multi-frequency Precise Navigation

A. Rovira-Garcia, J. M. Juan, J. Sanz
Research Group of Astronomy and Geomatics, Technical University of Catalonia, Spain, gAGE/UPC

BIOGRAPHY

Mr. A Rovira-Garcia is a PhD candidate at gAGE/UPC. His research is focused in enhanced algorithms of the Fast Precise Point Positioning (Fast-PPP) technique.

Dr. J.M. Juan Zornoza is senior researcher at gAGE/UPC. His current research interests are in the area of GNSS data processing Algorithms for High Accuracy GNSS Navigation and GNSS ionospheric sounding, as well as Augmentation Systems (SBAS and GBAS).

Dr. J. Sanz Subirana is senior researcher at gAGE/UPC. His current research interests are in the area of GNSS data processing algorithms, GNSS ionospheric sounding, augmentation systems (SBAS and GBAS), and High Accuracy GNSS Navigation.

ABSTRACT

The ionosphere plays an important role in satellite-based navigation, either in standard navigation, with single frequency mass-market receivers, or in precise navigation, with dual frequency receivers.

In this work, the requirements of a real-time ionospheric model suitable for GNSS applications are explored, in terms of accuracy and confidence bounds. Key factors for an ionospheric determination better than 1 Total Electron Content Unit (TECU) (16 centimeters in L1) are shown to be whether the model has been derived using an ambiguity-fixing strategy and the number of layers used to reproduce the ionospheric delay. Different models are assessed both in mid-latitudes and equatorial regions, near the Solar Cycle maximum.

It will be shown how dual-frequency users take benefit from a precise modelling of the ionosphere. If accurate enough, the convergence of the navigation filter is reduced to achieve high accuracy positioning quickly, (i.e., the Fast Precise Point Positioning technique). Satellite orbits and clocks computed for Fast-PPP will be shown to be accurate to few centimeters and few tenths of nanoseconds, respectively.

Single-frequency users correct its measurements with the predictions provided by any ionospheric model. Thence, the accuracy of the Fast-PPP ionospheric corrections is directly translated to the measurements modelling and, consequently, to the user solution.

Horizontal and vertical 95% accuracies are shown to be better than 36 and 63 centimeters for single-frequency users and 11 and 15 centimeters for dual-frequency users. The assessment is done for several locations, including the equatorial region, for a month of data close to the last Solar Maximum. The trade-off between the formal and actual positioning errors has been carefully studied by means of the Stanford plots to set realistic confidence bounds to the corrections.

INTRODUCTION

Precise Point Positioning (PPP) is a technique [1] for achieving high-accuracy positioning, typically sub-decimeter level in kinematic mode, for any world-wide user with a dual-frequency GNSS receiver. PPP is based on using satellite orbits and clocks more accurate, few centimeters, than those broadcast by the GNSS satellites. In order to compute them, data from a global network of permanent receivers, e.g., the International GNSS Service (IGS) [2], must be accurately modeled and processed by a Central Processing Facility (CPF).

PPP users eliminate the 99.9% of the ionospheric error in the GNSS signals thanks to the dual-frequency ionospheric-free combination of code and carrier-phase measurements. However, the noise of the raw GNSS measurements is amplified in this combination (a factor 3 using L1 and L2 signal bands). Moreover, carrier-phase ambiguities are estimated as real numbers (floated ambiguities) instead of integers (fixed ambiguities). These are clear drawbacks compared with the classical Real Time Kinematic (RTK) technique [3] which works in differential positioning up to some tens of kilometers from a reference receiver.

As a result, PPP requires more time than RTK to achieve high-accuracy navigation. Indeed, the floated carrier-phase ambiguities are separated (decorrelated) from the other parameters only when there is a significant change in the satellites-receiver geometry, which occurs after the best part of one hour. This convergence time can be shorter using low noise pseudoranges and/or using observations from more satellites (i.e., in a multi-constellation environment).

Some authors proposed in [4], [5], [6] a PPP service with the added capability of undifferenced ambiguity fixing to enhance the accuracy of the navigation. Finally, the convergence time is shortened in [6] with a continental enhancement based on precise ionospheric corrections. This last technique, named Fast-PPP is protected by several international patents [7] funded by the European Space Agency (ESA).

In this work, we will present the implementation of the Fast-PPP ionospheric model at a global scale. This is a requirement in the ESA funded project ICASES [8], which has supported the best part of this activity. On a daily basis, reference ionospheric values are computed thanks to the precise modeling of measurements done in the Fast-PPP CPF. Besides ionospheric estimates, precise satellite orbits and clocks, fractional part of ambiguities, Differential Code Biases (DCBs), are also determined.

The paper is divided as follows: in the next section we will describe how the Fast-PPP CPF is implemented and we will list the corrections routinely produced. The accuracy of the different corrections will be assessed in the 3rd section, paying special attention to those related with the ionospheric modeling. In the 4th section we will show how, using these accurate corrections, the navigation of any user improves. This is done not only for users with a dual frequency GNSS receiver but also for rovers with single frequency receivers. Moreover, we will show that the results on navigation are reliable, thanks to that the CPF not only computes the corrections but also their confidence bounds. Finally, the last section will summarize the results.

FAST-PPP IMPLEMENTATION

Fast-PPP corrections for high-accuracy navigation are computed in a unique Central Processing Facility (CPF), with multi-frequency and multi-constellation capabilities. The estimation of the different corrections is done thanks to a multi-filter strategy, where each filter works with a different updating time (see [6] for more information).
The CPF is fed by the data gathered by three different sets of GNSS receivers (see an example in Figure 1). The first network (shown in black) includes all receivers. Data are processed in order to obtain the satellite orbit corrections and the satellite fractional part of ambiguities every 5 minutes. A second network of receivers (the blue subset of the previous one) is used to estimate the satellite clocks, which in this implementation is done with a faster rate of 30 seconds.

Finally, a third ionospheric sub-network (red) is used to estimate the parameters of an ionospheric model. In this implementation, it covers a longitude range from -130 to 130 degrees and a latitude range from -90 to 90 degrees. The ionospheric model consists on a two-layer [9] irregular grid model where the distance between Ionospheric Grid Points (IGP) is maintained to be around

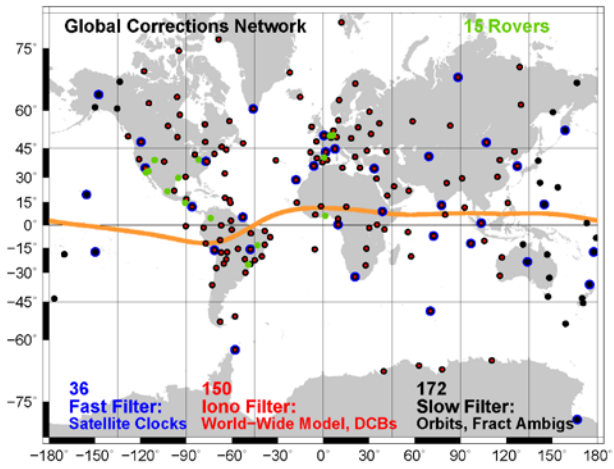

Figure 1: Distribution of rovers (green) used in this study during days 169-200 of 2014. All reference stations (black) are used to calculate orbit corrections, and fractional part of the ambiguities. The blue subset of stations is used to compute satellite clocks and the red to derive the ionospheric model. The geomagnetic equator is shown in orange.

250km. The CPF updates the Total Electron Content (TEC) values of the IGPs and satellite DCBs every 5 minutes.

Besides the three mentioned networks, a set of receivers is navigated as rovers in order to assess the CPF products. These receivers are world-wide distributed (shown as green dots in the map), covering in particular the regions served by the current augmentation systems and their planned extensions. Distances from these rovers the nearest ionospheric reference station range from one to eight hundred kilometers, which is more than one order of magnitude greater than the Real Time Kinematics (RTK) or Network-RTK [10] baselines.

FAST-PPP CPF CORRECTIONS ASSESSMENT

As stated in the introduction, the Fast-PPP CPF is running, in an automatic way, every day since the beginning of 2014. In this section, we will do an assessment of the quality of the corrections computed by the Fast-PPP CPF for the range of days from 169 to 200 (i.e. a month of data). The period is close to the Solar Cycle maximum according to the solar flux shown in Figure 2 (top), but the geomagnetic activity reported by the Dst index [11] is quite moderate (Figure 2, bottom).

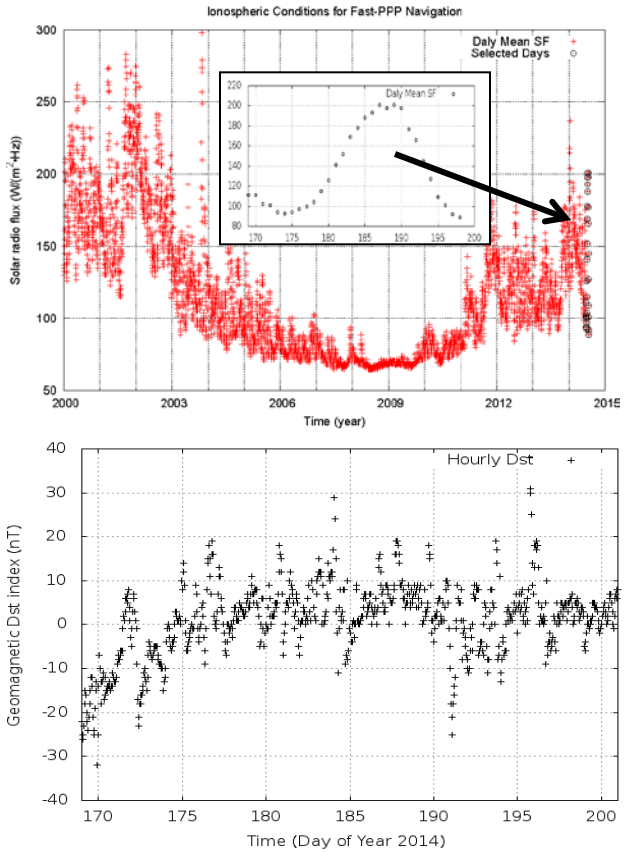

Figure 2: Radio solar flux (top, red) since 2000 with a zoom (top, black) for the selected period (days 169-200 of 2014). The bottom plot shows in black the geomagnetic disturbance index Dst only for the studied days.

Fast-PPP Satellite Orbits

The Fast-PPP CPF orbit correction module can work from broadcast or IGS orbits. Because the mentioned ICASES project targets periods of high ionospheric activity with variations up to several meters in 30 seconds, classical cycle slip detectors based on a smooth ionosphere cannot be used. Indeed, special cycle slip detectors have been developed that require previously estimated orbits and clocks from, for instance, IGS rapid products (IGR) to build the prefit measurements without flagging false detections. For this reason, in ICASES, no orbit corrections are estimated by the Fast-PPP CPF. However, in order to show that we don't take any advantage of using IGR orbits, some days (the first week) have been also processed using the predicted part of the ultra-rapid IGS orbits (IGU). These orbits are adjusted in the Fast-PPP CPF. Results show no significant differences regarding to the IGR products.

In Figure 3, the Root Mean Square (RMS) of the 3D orbit differences between the IGU orbits and the IGR orbits is shown in black. It is evident the degradation of the IGU orbits as they become "older". In contrast, IGU orbits corrected by the CPF in real-time, mitigate the orbit degradation until a new orbit prediction set is delivered every 6 hours. In this regard, the RMS of the orbit error is 4.3 cm, in line with other centers that compute satellite orbits in the IGS Real-time Pilot Project (IGS-RTPP) [12].

Fast-PPP Satellite Clocks

Unlike with satellite orbits, the Fast-PPP CPF always estimates satellite clocks regardless of the orbit source. The assessment of the satellite clock corrections product can be done by comparing directly with the IGR clocks. In Figure 4, it is shown the RMS of the difference between the IGR clocks and the Fast-PPP clocks (red). In this plot we have included the same comparison when the Fast-PPP CPF starts from the predicted part of the IGU orbits (blue). It can be seen that both orbit sources produce similar satellite clock corrections, even slightly better when the orbits are corrected. In both cases the RMS is around 0.2 ns, which is in line with the performance obtained by other analysis centers of the referred IGS-RTPP [12], for the clock product.

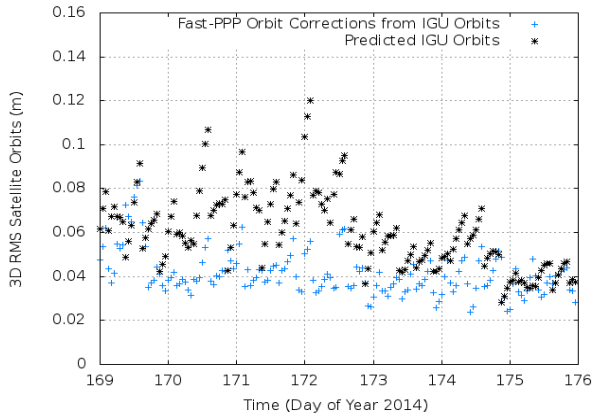

Figure 3: RMS of the 3D orbit difference with respect to the IGS rapid orbits (IGR) for days 169-176 of 2014. Fast-PPP CPF computes real-time orbit corrections (blue) to the predicted IGS ultra-rapid orbits (IGU) shown in black.

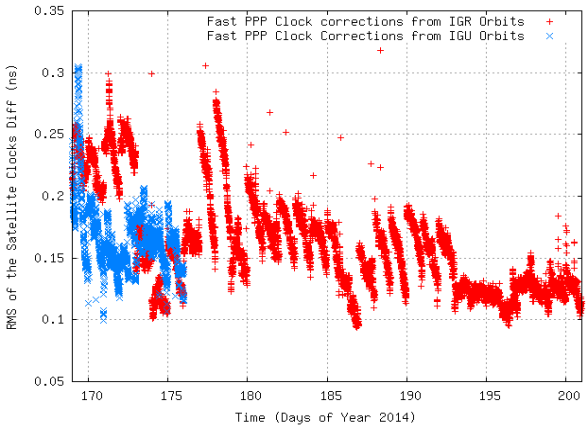

Figure 4: RMS of real-time satellite clock corrections with respect to the IGS rapid clocks for days 169-200 of 2014. Fast-PPP CPF can compute the satellite clocks either from predicted IGS ultra-rapid orbits (IGU) (blue) or from post-process IGS Rapid orbits (IGR), shown in red.

Fractional part of the ambiguities

PPP users can enhance their positioning by fixing carrier-phase ambiguities to integer values. This can be done in undifferenced mode and on a world-wide basis, thanks to the CPF capability of estimating the satellite fractional part of the ambiguities [4], [5], [6]. Although there is not a standard product to be used as reference and the value depends on the reference taken in the CPF, the agreement between independent estimations (i.e., consecutive days) can be assessed, as in Figure 5, where the values for three representative satellites are depicted.

Figure 5 shows the fractional ambiguities for of L1 band, (B1, top), and the Wide-Lane combination, (BW, bottom), computed using both the IGR and the IGU corrected orbits. From these plots, it follows: i) they are slow-varying parameters, and thence, can be broadcast to users with a large time update (e.g. every 5 minutes in this implementation) ii) the fractional B1 ambiguity discontinuities on a day-to-day basis are typically smaller than a 0.1 cycle (2 cm) when IGU orbits are corrected. iii) the consistency of B1 is slightly degraded when IGR orbits are used (disabling the orbit correction module), indicating that some residual orbit error is transferred to the ambiguity estimation. iv) the repeatability of the BW fractional ambiguity does not depend on the orbit source.

At user level, the satellite fractional part corresponds to the term δB^j in equation (1) for an ambiguity B_i^j for a particular frequency (and corresponding wavelength, λ) between a receiver i and a satellite j. The receiver fractional part δB_i is common to all satellites sharing that frequency.

$$B_i^j = \lambda N_i^j + \delta B_i + \delta B^j \quad (1)$$

The ambiguity fixing strategy is given by equation (2), where the receiver fractional part is eliminated by differencing with respect to a reference satellite B_i^0 (usually the highest). The satellite contributions are removed with the CPF correction ($\delta B^i, \delta B^0$).

$$\left(B_i^j - \delta B_{corr}^j\right) - \left(B_i^0 - \delta B_{corr}^0\right) = \lambda\left(N_i^j - N_i^0\right) \quad (2)$$

Three simultaneous conditions are required to be fulfilled before the Fast-PPP user fixes the ambiguities. (i) the formal error of the floated ambiguities $\left(B_i^j, B_i^0\right)$ has to be under a certain threshold. (ii) the left hand side of equation (2) divided by λ must be close enough to an integer. (iii) a minimum number of epochs since last cycle-slip of the arch are also required. When these tests are successful, the term $\left(N_i^j - N_i^0\right)$ is fixed to an integer value. Thence, the constraint of equation (2) is added to the navigation filter with a great confidence (low sigma).

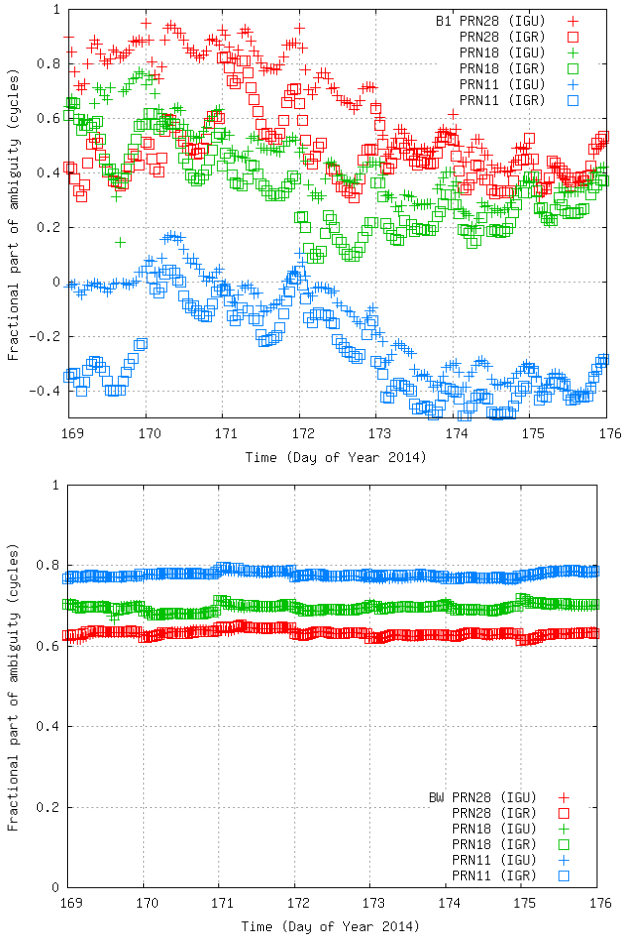

Figure 5: Satellite fractional part of the ambiguities in cycles (B1: top, Wide-Lane (BW) combination: bottom) using two type of IGS orbit sources: IGR (squares) and IGU (pluses).

Satellite Differential Code Biases

The determination of the satellite Differential Code Biases (DCBs) is a key factor for users applying ionospheric corrections; otherwise, those biases would worse the user positioning (especially the single-frequency). The DCB can be accurately estimated from pseudorange measurements by mixing rays at several (globally) different local times and the ionospheric model. Although codes are about two orders of magnitude noisier than the carriers, all observations from the same satellite (or receiver) have the same DCB. This high redundancy allows the Fast-PPP CPF to estimate them with a high consistency on a day to day basis, as it is shown in the top plot of Figure 6, over a month (days 169-200 of 2014). After a convergence time of several hours, DCBs are typically determined with a standard deviation at the level of 0.02 meters of L1-L2, as it is shown in Figure 6 (bottom).

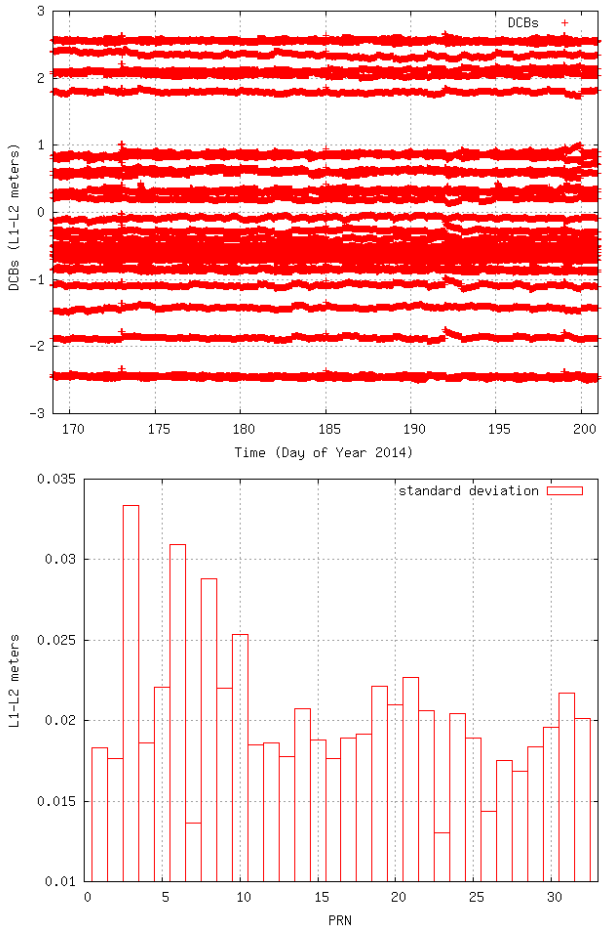

Figure 6: Satellite Differential Code Bias (DCB) estimation (top) and the standard deviation (bottom, in function of PRN).

Fast-PPP Ionosphere

The core of the Fast-PPP is the real-time determination of the ionospheric delay present in the GNSS signals, Slant TEC (STEC). Its accuracy is at the level or better than 1 Total Electron Content Unit (TECU), which corresponds to 16 centimeters in L1. The left hand of (3) is the unambiguous geometry-free ($LI = L1 - L2$ [13]) combination of carrier-phase measurements LI_i^j for the satellite "j" and receiver "i". Once the carrier-phase ambiguity of this combination BI_i^j is corrected, thanks to the Fast-PPP CPF accurate geodetic modeling that allows its fix.

$$LI_i^j - BI_i^j = STEC_i^j + DCB_i - DCB^j \qquad (3)$$

In the right hand side, satellite DCB^j and receiver DCB_i are separated from the ionospheric delay$STEC_i^j$. This STEC can be expressed as a lineal combination of the Vertical TEC (VTEC) on each "k" Ionospheric Grid Point (IGP) following (4). Where α_k is a geometric factor which includes the obliquity factor and the geometric interpolation from the IGPs of each layer:

$$STEC_i^j = \Sigma\, \alpha_k \cdot VTEC_k \qquad (4)$$

The Fast-PPP CPF estimates, every 5 minutes in this implementation, the vertical ionospheric delays $VTEC_k$ and the DCBs. A constant 250 and 500 kilometers spatial resolution in latitude and longitude is used, in the first (main ionosphere) and second layer (plasmasphere), respectively.

Ionospheric model assessment

The assessment of the accuracy of any ionospheric model for GNSS navigation is an open problem because, unlike of satellite orbits and clocks, there is not any reference ionospheric model with the required accuracy (i.e. at the level of 1 TECU). For this reason, we have developed a test using as a reference value the unambiguous determinations ($STEC_{true}$) computed by the CPF, according to the equation (5):

$$STEC_{true,i}^j = LI_i^j - BI_i^j - (DCB_i - DCB^j) \qquad (5)$$

The $STEC_i^j$ values derived from equation (5) can be thought to represent the true value, ($STEC_{true}$), except for a bias originated due to inaccuracies in the DCB estimates. Thence, the difference between the prediction of any ionospheric model and the reference should be separated as DCBs in (6) (i.e. a constant for the receiver K_i plus a constant for the satellite K^j):

$$STEC_{model,i}^j - STEC_{true,i}^j = K_i + K^j \qquad (6)$$

The K_i and K^j on the right hand of the previous equation are estimated by a Least Minimum Squares (LMS) process. The post-fit residuals of this adjustment provide a metric to assess the realism of the STECs predicted by the ionospheric model. Notice that any common bias in the STECs affecting both satellites and/or receivers will not affect the test result, since it is absorbed into the receiver and satellite constants. In this sense, this test assesses the ionospheric predictions of any model in a global scale, because K_i and K^j are set as common constant parameters for the entire network of receivers (and satellites) and over the data interval.

The RMS of the residuals from the fit using equation (6) is shown in Figure 7 for all reference stations used by the ionospheric filter. Fast-PPP ionospheric estimates in real time (black) present the best agreement with respect to unambiguous STECs. Fast-PPP ionospheric model is limited to the regions where data is available in real-time, there are not estimations for IGPs on poor sounded areas (i.e., the oceans). In order to build a Global Ionospheric Map (GIM), these IGPs must be also estimated, using a

smoothing process that degrades the well-sounded IGPs. This partially explains the large improvement of the real-time Fast-PPP ionospheric model respect the IGS GIM.

Then, a more fair comparison is also included in Figure 7 after smoothing (in post-process) the Fast-PPP ionospheric model, which leads to the Fast-PPP GIM shown in blue. The Fast-PPP GIM maintains the error at the level of 1 TECU. This figure is several times better than the rapid (red) IGS GIM, with a nominal accuracy of 2-8 TECU in vertical [14]. The difference between GIMs can be partially explained by the ambiguity-fixing strategy of the Fast-PPP. Both GIMs follow a daily periodicity following the local time (top plot) and a monthly variation related with the solar radio flux shown in the zoom of Figure 2, (top plot).

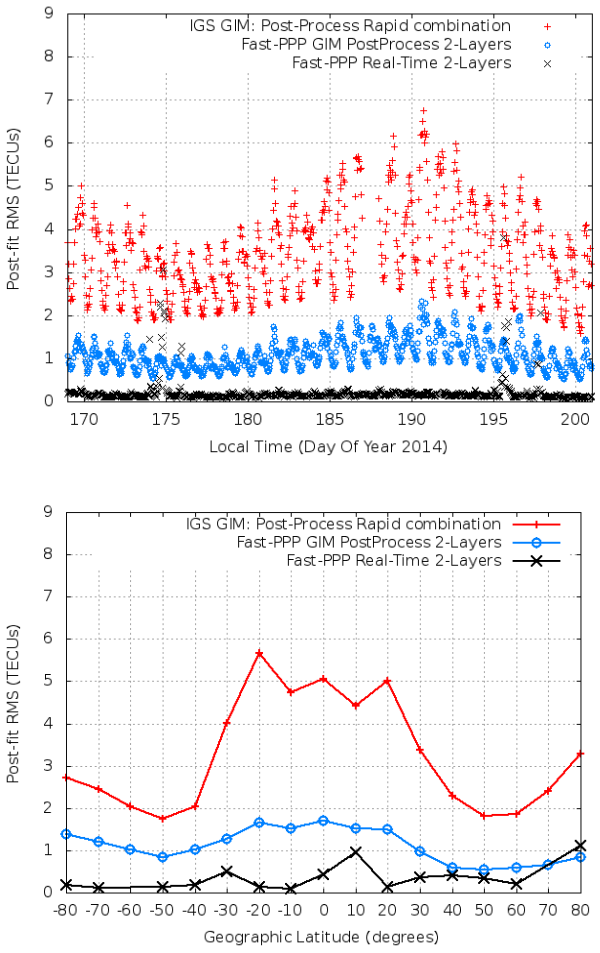

Figure 7: Results of the consistency test between different ionospheric estimates; 2-h GIM IGS combined rapid product (red), a 15-minute GIM delivered to ICASES project (blue), and the real-time 5-minute Fast-PPP ionosphere using two layers (black). The horizontal axis is the local time in the top plot and latitude in the bottom plot.

Another major advantage of the Fast-PPP ionospheric model is the use of a dual-layer strategy to separate the main ionosphere and the plasmasphere. Each component has a different height and dynamic evolution. This difference in the model geometry is more noticeable when RMS test results are compared on a latitude basis, bottom plot of Figure 7. It can be clearly seen that the equatorial region cannot be described accurately with a single-layer approach (IGS-GIMs).

It must be pointed out that the IGS GIM is updated every 2 hours, the Fast-PPP GIM is updated every 15 minutes and the Fast-PPP real-time every 5 minutes. Nevertheless, although the lower time update contributes to reduce the error, the key factor improving the accuracy is the processing strategy as a whole (i.e., the two ionospheric layers, the grid size and, remarkably the use of the fixed ambiguities as constrains in the filter).

FAST-PPP NAVIGATION

The Fast-PPP user navigation strategy keeps code and carrier phase measurements (L1, L2, P1, P2) separate from the previously explained CPF corrections. These are included in the navigation filter as additional equations with their confidence bounds (sigmas). This is a similar approach than [15] but in absolute mode. In this sense, not only the accuracies of the corrections are relevant, but also their confidence bounds. Less accurate corrections as a result of a poor estimation, network outage, satellite eclipses or ionospheric events do not worse the user positioning since they are bounded by large sigmas.

In this section, it is shown the user positioning achieved by the current implementation of the Fast-PPP technique, using the real-time Fast-PPP ionosphere. First, it will be shown how the accurate geodesy corrections (satellite orbits and clocks) computed by the CPF, enable a highly accurate navigation for single- and multi-frequency users, regardless of the orbit source (IGR or IGU). After this, the real-time ionospheric corrections will be proven to shorten the convergence time to achieve such precise positioning (i.e., Fast-PPP). The improvement is measured with respect to the current ionospheric-free navigation techniques; the Group and Phase Ionospheric Calibration (GRAPHIC) [16] and Precise Point Positioning (PPP) [1] techniques, for single and dual frequency users respectively. Finally, the Stanford plots are used to assess how the Signal-In Space (SIS) confidence bounds are transferred to the user domain, showing the internal consistency of the parameterization and hypothesis done in the Fast-PPP navigation, achieving adequate protection levels.

Orbit Corrections Assessment

The impact on the position domain of using the Fast-PPP corrections computed from the rapid orbits without correcting them or correcting the predicted products is assessed in Figure 8. It is shown the merged 3D RMS error of all rover solutions for one week (DOYs 169-176 in 2014), resetting the filter state every two hours. The black curves correspond to the navigation achieved using IGU orbits, while the color dots correspond to navigation using IGR orbits. It can be seen that both orbit sources provide similar results for the ionosphere-free solutions (GRAPHIC, PPP) and the ionospheric solutions (Fast-PPP), in single and dual frequency navigation modes. Thence, it is also confirmed at the user domain, that no benefit is taken from computing the Fast-PPP corrections using the post-process IGR rapid orbits from IGS.

Convergence Assessment

The reduction of the convergence time of the user positioning by means of ionospheric modelling is seen after a user cold start or a cycle slip. The carrier-phase ambiguity estimation is shortened by the Fast-PPP ionosphere, which is absolute (i.e., unambiguous) and several times more precise than the code measurements. Otherwise, in PPP or GRAPHIC, ambiguities are mostly estimated with the noisy (although unambiguous) code. The relation between the ionospheric performance of Figure 9 and the convergence of the rovers of Figure 10 will be explained next.

The efficiency of the ionospheric corrections decreases with the error of the ionospheric model once it its interpolated by the user. Note that the postfit test presented in previous Figure 7 at the reference stations is the minimum error that the ionospheric model has by the fact of representing un-ambiguous STECs by means of a

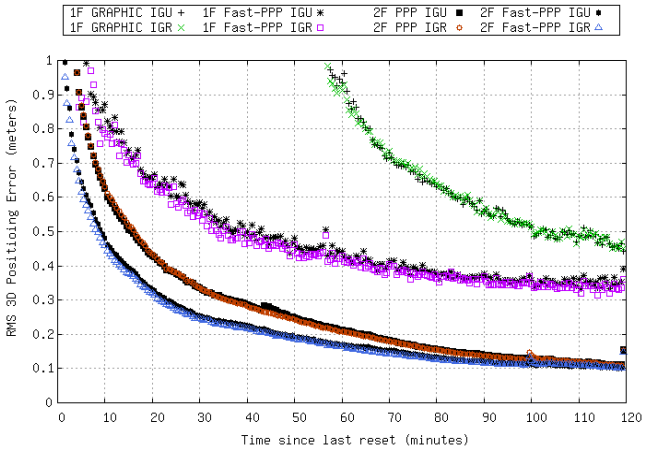

Figure 8: RMS of the 3D error as function of the elapsed time since the receiver is reset (every 2 hours). Curves involve all rovers present in days 169-176 of 2014 for both orbits sources: predicted IGU (black) and rapid IGR (color).

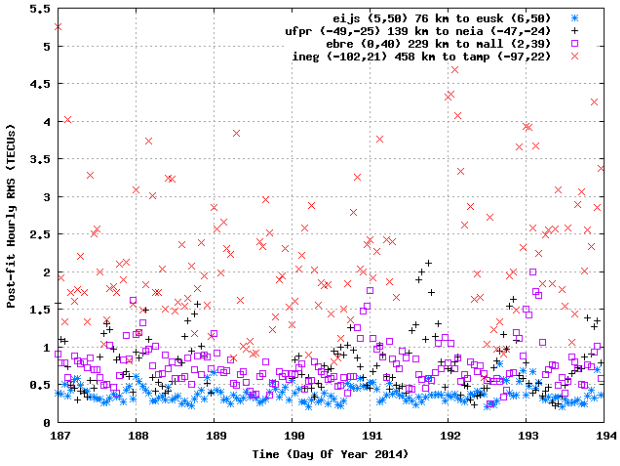

Figure 9: RMS of the real-time, two-layer Fast-PPP ionospheric estimates for some rover locations, located at different distances from nearest reference station.

grid. The second source, the interpolation contribution, will depend on; (i) the ionospheric activity shown in Figure 2, (ii) the distance to the stations which are used to derive the ionospheric model, (iii) the user latitude.

Figure 9 presents the postfit test at different rover locations and distances during the maximum solar flux of the period. It can be seen, that in mid-latitudes the degradation is small: Up to 100 km (eijs) the error is at the same level than a reference station (0.5 TECUs). The interpolation error gets larger with increasing distances, but it is kept to a 1 TECU level at a few hundreds of kilometers (ebre). At low latitudes, the degradation is more noticeable with respect to distance (ufpr), and at 140 km the error already is at 1 TECU level.

This ionospheric performance is translated to the user positioning shown in Figure 10, where Fast-PPP single frequency performance since the beginning of a cold start with 30 and 70 centimeters of horizontal and vertical accuracies, respectively. After 30 minutes, errors are reduced to 20 and 40 centimeters. Final converged values after one hour present 20 and 30 centimeters of horizontal and vertical accuracy, respectively. These figures are several times better than for GRAPHIC positioning (i.e., without using ionospheric corrections). Fast-PPP dual frequency users reduce the PPP convergence time needed to achieve a navigation error below 1 decimeter between 80% to 60% in the horizontal component and 60% to 30% in the vertical component.

The degradation with respect to increasing distances can be appreciated in the plot for rover lkhu. Single-frequency horizontal and vertical initial accuracy worsens to 40 cm and meter-level positioning. Fast-PPP ionosphere keeps reducing the GRAPHIC convergence time, reaching the same 20 and 30 centimeters, respectively. In dual-frequency, Fast-PPP still marginally reduces the PPP convergence time.

The largest error, up to several TECUs, occurs at rover ineg. Not only because its equatorial location, but also because it is located at 460 km and 1400 km of the two nearest reference stations. At user level, it is shown no advantage of using Fast-PPP ionospheric corrections Thanks to the confidence levels (sigmas) of the ionospheric corrections, used as weights in the navigation filter, Fast-PPP user solutions never worse GRAPHIC or PPP.

The convergence assessment confirms the Fast-PPP precise ionospheric modelling added to the navigation filter is translated into the user positioning resulting in a quicker convergence, leaving the final (once converged) accuracy untouched thanks to the unbiased nature of the Fast-PPP ionosphere. Moreover, results indicate that a denser network shall be used in the equatorial region to keep the ionospheric error at 1 TECU level, and thence, the user domain performance observed in mid-latitudes.

In all cases analyzed in Figure 10, we have included the results using the ionospheric corrections from the rapid GIM from IGS for both single and dual frequency navigation modes. As one can see, the improvements are not maintained with these corrections, even occurring a worsening of classical ionosphere-free solutions.

Actual vs Formal Errors Assessment

The reliability of the Fast-PPP technique at user domain is shown in Figure 11, comprising the entire rover network for the period (DOYs 169-200 in 2014). Stanford plots assess horizontal (left) and vertical (right) components, and the dual-frequency (top) and single-frequency (bottom) navigation modes. Every 24 hours of data are processed independently without resetting the rover. Vertical and horizontal protection levels (VPL and HPL) are computed as VPL $=5.33\sigma_v$ and HPL $=6.00\sigma_h$. The values 5.33 and 6.00 are the K-factors associated with probabilities of Misleading Information (MI) of 10^{-7} and $2 \cdot 10^{-9}$, see appendix J of [17].

Horizontal and vertical 95% accuracies are 15 and 63 centimeters for single-frequency users and 11 and 36 centimeters for dual-frequency, respectively. More important, such figures are achieved with safe margins between actual and formal errors thanks to: (i) the confidence bounds associated to the CPF corrections (satellite clocks, ionosphere, DCBs) and (ii) the realism of the a-priory hypothesis assumed (standard deviations of pseudorange and carrier-phase prefit measurements) and the troposphere rate. Relative weights are key for the navigation filter to mix correctly such different information.

CONCLUSIONS

An end-to-end performance assessment of the Fast-PPP technique at a planetary scale has been presented. The accuracies of the CPF real-time precise satellite orbits and clocks have been shown to be of the order of IGS real-time products, respectively, a few centimeters and a few tenths of a nanosecond. This global PPP service is enhanced by Fast-PPP with the added capability of global undifferenced ambiguity fixing thanks to the estimate of the fractional part of the ambiguities.

Once satellite orbits and clocks that are accurate to some centimeters are made available to users in real time, the remaining challenge is the computation of an accurate ionospheric model to enhance performances of both dual- and single- frequency PPP users. A dedicated metric has been introduced to assess the suitability of ionospheric models for high-accuracy navigation. It has been shown that the two-layer, ambiguity-fixed Fast-PPP ionospheric real-time estimates are typically accurate to less than 1 TECU (16 centimeters in L1) and can be used in combination with precise orbits and clocks maintaining their accuracy. This is not the case for the well-known IGS GIMs, with accuracies several times worse. It has been shown that the contrast between the two ionospheric models is greater at low latitudes and around local noon.

Fast-PPP dual-frequency users benefit from the precise ionospheric modeling through a several-fold reduction in the convergence time compared to the classic PPP solutions, not only in mid-latitude regions but also under more challenging ionospheric conditions such as those found in the equatorial region. This is noticeable for rover baselines up to 500 kilometers, which makes the technique feasible using a sparse reference station network. Further or isolated rovers only allow a slight improvement, never producing poorer results than the ionosphere-free solutions, thanks to the realism of the Fast-PPP correction confidence levels calculated at the CPF level.

Finally, it has been shown that accuracies of single-frequency users are directly affected by the quality of the ionospheric estimates. Out results show the improvement in the Fast-PPP ionospheric model compared to IGS GIMs, especially at low latitudes. On a planetary scale, navigation of users with mass-market receivers is safely bounded under protection levels of the order of a meter.

ACKNOWLEDGMENTS

This work has been partially sponsored by the ESA Network Partner Initiative (NPI) with the industrial partner FUGRO. The Technical University of Catalonia contributed with a FPI-UPC grant. We also would like to thank to the Spanish Ministry of Science and Innovation project CTM2010-21312-C03-02 and the GNAVIS project from EC-FP7 Grant Nr. 287203. The activity has been developed for the ESA funded project ICASES [8].

REFERENCES

1. *Precise point positioning using igs orbit and clock products.* **Heroux, J. and Kouba, P.** No. 2, 2001, GPS Solutions, Vol. 5, pp. 12–28.

2. *The International GPS Service (IGS): An interdisciplinary service in support of Earth sciences.* **R. Beutler, M. Rothacher, S. Schaer, J. Kouba, and R. Neilan.** No 4, 1999, Advances in Space Research, Vol. 23, pp. 631–653.

3. *Performing centimetre Accuracy Relative Surveys in Seconds Using GPS Carrier Phase on Precise Positioning with the Global Positioning System.* **Remond, B. W.** Rockville, MD : s.n., 1985. First International Symposium. pp. 361–377.

4. *Integer Ambiguity Resolution on Undifferenced GPS Phase Measurements and Its Application to PPP.* **Mercier, D. and Laurichesse F.** Fort Worth, TX, USA : s.n., 2007. Proceedings of ION GNSS 2007. pp. 839 - 848.

5. *Resolution of GPS Carrier-Phase Ambiguities in Precise Point Positioning (PPP) with Daily Observations.* **M. Ge, M. Gendt, M. Rothacher, C. Shi, and J. Liu.** 2008, Journal of Geodesy, Vol. 82, pp. 389–399.

6. *Enhanced Precise Point Positioning for GNSS Users.* **M. Juan, M. Hernández-Pajares, J. Sanz, P. Ramos-Bosch, A. Aragon- Angel, R. Orus, W. Ochieng, S. Feng, P. Coutinho, J. Samson, and M. Tossaint.** 10, 2012, IEEE Transactions on Geoscience and Remote Sensing, Vol. 50, pp. 4213–4222.

7. **Hernández-Pajares, M., Juan, M., Sanz, J., J. Samson, and M. Tossaint.** *PCT/EP2011/001512* Method, Apparatus and System for Determining a Position of an Object Having a Global Navigation Satellite System Receiver by Processing Undifferenced Data Like Carrier Phase Phase Measurements and External Products Like Ionosphere Data, 2011.

8. ICASES: Ionospheric Conditions and Associated Scenarios for EGNOS Selected from the last Solar Cycle. European Space Agency (ESA) PO 1520026618/01. Noordwick, The Netherlands : s.n., 2014.

9. *A Two-Layer model of the Ionosphere using Global Positioning System data.* **Juan J.M., Rius A., Hernández-Pajares M., and Sanz J.** 1997, Geophysical Research Letters, Vol. 24, pp. 393-396.

10. *Reducing Distance Dependent Errors for Real Time Precise DGPS Applications by Establishing Reference Station Networks.* **G. Wubbena, A. Bagge, G. Seeber, V. Boder, and P. Hankemeie.** Kansas City, MO : s.n., 1996. Proceedings of ION GPS 1996. pp. 1845–1852.

11. *Dst as an Indicator of Potential Threats to WAAS Integrity and Availability.* **S. Datta-Barua, T. Walter, E. Altshuler, J. Blanch, and P. Enge.** Long Beach, California : s.n., 2005. Proceedings of ION GNSS 2005. pp. 2365–2373.

12. International GNSS Service Real Time Pilot Project (IGS-RTPP). [Online] 2007. http://www.rtigs.net/.

13. **J. Sanz, J. Juan, and M. Hernández-Pajares.** *GNSS Data Processing, Vol. I: Fundamentals and Algorithms.* Noordwijk, the Netherlands : ESA Communications, ESTEC TM-23/1, 2013.

14. **Service, International GNSS.** IGS Products. [Online] http://igs.org/components/prods.html.

15. *The geometry-free GPS ambiguity search space with a weighted ionosphere.* **Teunissen, P.J.G.** 1997, Journal of Geodesy, Vol. 71, pp. 370-383.

16. *Coping with the atmosphere and ionosphere in precise satellite and ground positioning.* **Yunck, T.** 1993, Environmental Effects on Spacecraft Trajectories and Positioning, pp. 1-17.

17. **Radio Technical Commission for Aeronautics.** *Minimum Operational Performance Standards for Global Positioning System/Wide Area Augmentation System Airborne Equipment.* Washington, USA : s.n., 2006.

18. **Products, IGS.** [Online] http://igs.org/components/prods.html.

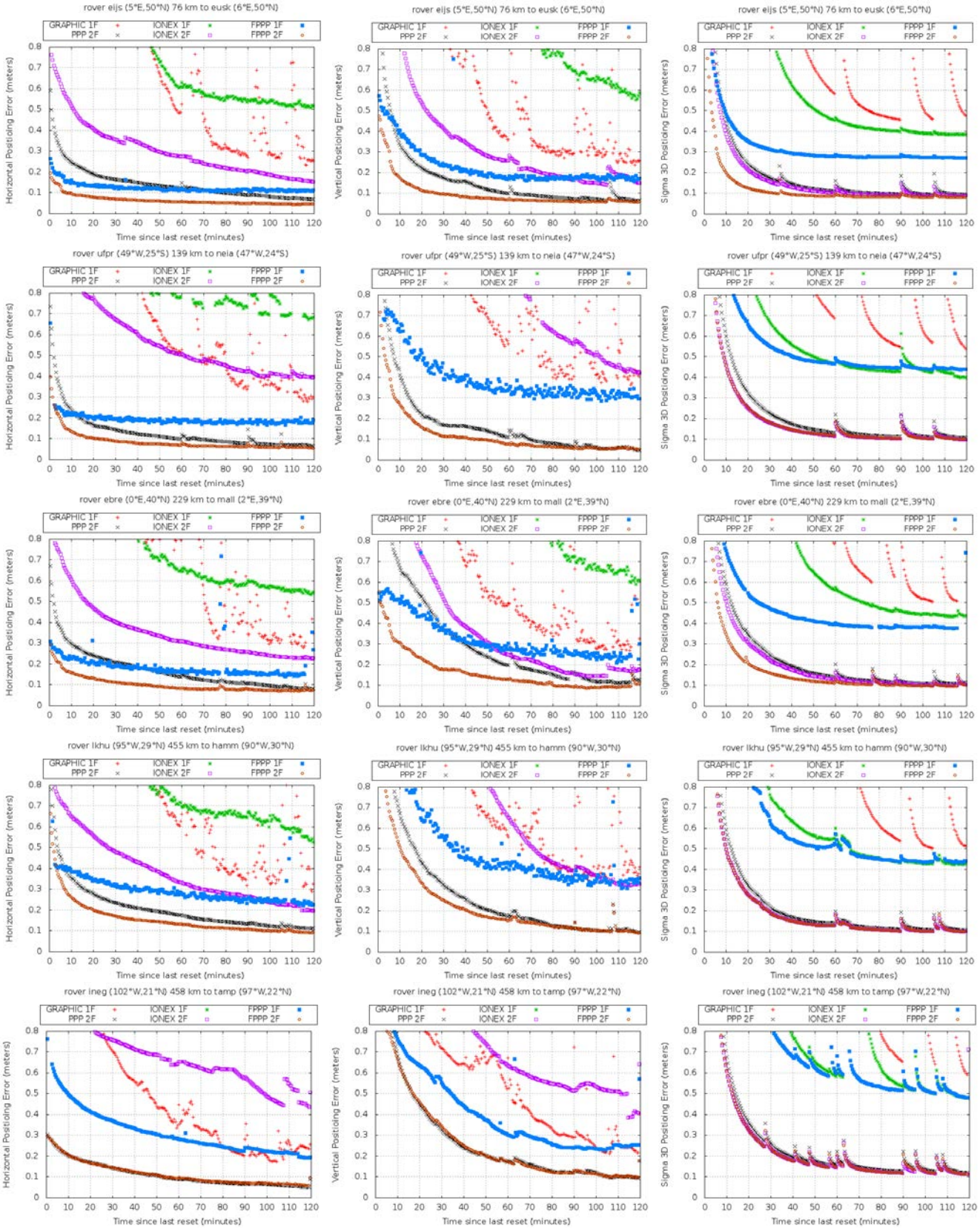

Figure 10: Horizontal (left) and vertical (center) RMS accuracies as a function of time since the receiver is reset every 2 hours, in days 169-200 of 2014. The right column shows the 3D positioning formal error. Single and dual frequency ionosphere-free solutions (GRAPHIC and Classic PPP) are compared with the ionosphere real-time of Fast-PPP and the post-processed IGS-GIMs.

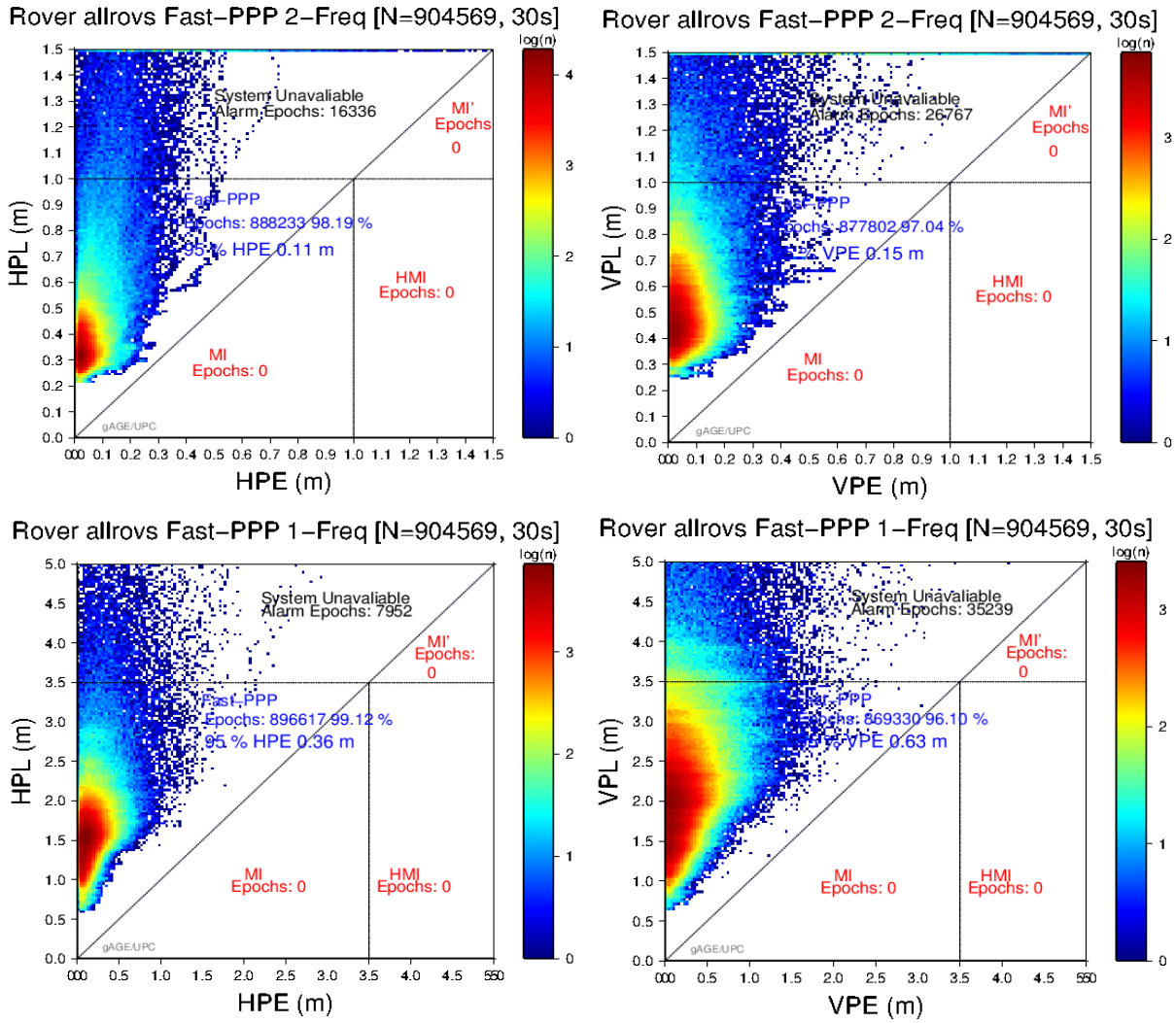

Figure 11: Protection Levels: horizontal (left) and vertical (right) Stanford plots for dual-frequency (top) and single-frequency (bottom) navigation solutions in days 169-200 of 2014 for all rovers merged in the same plot.